Solid Freeform Fabrication 2022: Proceedings of the 33rd Annual International
Solid Freeform Fabrication Symposium – An Additive Manufacturing Conference
Reviewed Paper

# RHEOLOGICAL CHARACTERIZATION OF ROOM TEMPERATURE POWDER METAL PASTE FOR EXTRUDED MATERIAL MODELING

Marshall Norris*, Ismail Fidan, Michael Allen
Tennessee Tech University
Cookeville, TN 38505

## Abstract

Powder metals have been used in Additive Manufacturing (AM) processes such as injection molding, extrusion, and slip casting for decades. Recent innovations in the Fused Filament Fabrication (FFF) have provided the opportunity to mix powder metals with a binding thermoplastic at elevated temperatures to create 3D components. This research attempts to define the rheological characteristics of paste materials used to produce 3D components at room temperature using powder metals that will provide the following three outcomes: material that will flow under low shear stress, green strength to provide structural support of material deposited on top and prevent deformation under gravitational load, and once cured to provide material properties that are comparable to those of materials produced by traditional means. The purpose of this research is to determine if powder metal components can be produced by FFF at room temperature while maximizing the powder metal composition in the mixture.

*Keywords:* Additive Manufacturing, Extruded Material, 3D Printing, Powdered Metal, Rheology

## Introduction

Powdered metals have been traditionally used to produce castings or injection molded components with a wide variety of characteristics. Recently, powdered metals have been used for 3D printing approaches based on laser scintillation (or laser powder fusion), Direct Energy Deposition (either laser based, plasma, e-beam, or electric arc), and binder jet fusing [1] [2]. With the increase in availability of FFF based printers, powdered metals have been investigated for use in FFF approach. One area of research is focused on the addition of fibrous materials to polymer FFF printing material such as carbon, glass, and Kevlar [3]. The area research includes the material characterization and generating models based on assumptions of homogeneity in the material which can accurately predict fiber and microstructure [4]. Further study has determined the influence of printing parameters such as raster angle, infill speed, layer thickness, and nozzle temperature on mechanical properties [5].

In popular FFF techniques, the powdered metal is added to the plastic filament and must behave as a liquid for a period and then transition to a solid that can support its own weight under gravitational loading. This is achieved when the powdered metal is mixed with a binding agent to create a 2-state material. The focus of this paper is on the characterization of powdered metal solutions in the first phase. While some FFF printers use a thermoplastic as a binding agent, this research is focused on FFF at room temperature using a paste of 316SS or carbon steel and liquefied polyvinyl acid (PVA) as a binding agent. The advantages of using this method are that the process is scalable, reduces or removes thermal stresses between vertical layers, and print speed can be increased by increasing the volumetric flow rate.

*Corresponding Author

For metal injection molding feedstocks, as the percent of powder metal is increased in the paste, flow changes from Newtonian to a strong shear thinning behavior [6]. However, for low shear rates, a Newtonian plateau is still observed. It was therefore hypothesized that if the shear rate, and consequently the material flow rate, remains low enough, the material will behave in a Newtonian manner. Using a low PVA to water ratio as shown by [7] will increase the linear behavior of the mixture.

The paste is used as feedstock for a hybrid FFF-injection molding printer that extrudes the material onto the bed of a modified FFF printer. A 3D model is used as an input to a program that creates a series of horizontal slices through the part and creates a path to trace the geometry, or "G-code", of each layer. The printer then extrudes each layer beginning at the lowest layer and prints each consecutive layer on top of the previous layer. Each layer of the paste dries and the final print is subjected to a heat treatment process which hardens the metal from a green state to a final state such that its properties are approximately equivalent to that generated by forgings or castings.

Two shapes of powder were used for this test, an irregular particle and a spherical powder. The end goal would be to fully characterize the spherical powder because the ability to maximize the density of the final printed product increases as the particles become more spherically regular and decrease in size.

## Background

Powdered metals can be created by chemical reaction, decomposition, electrolytic deposition, atomizing molten metals, and mechanical processing of solid materials which result in a wide variety of characteristics such as particle size and distribution, particle shape, surface area, inter-particle friction, flow and packing, internal particle structure, chemical gradients, surface films, and others [8]. Gas and centrifugal techniques, which produce spherical particles necessary for increased packing, produce similar constituent percentages to those of parent material. Particle size also plays an important role in the packing, this research targeting particle sizes of 15-45 μm. Material used in cold isostatic die compaction is premixed with lubricants and binding agents. Material used for this research is unmixed spherical 316L and irregular shaped premixed carbon steel.

During production, powdered metals are mixed with additives to a desired viscosity depending on the desired application method. The shear rate for gravity leveling (tape and slip casting) is on the order of $10^{-1}$ $s^{-1}$, while pumping, pouring and mixing are on the order of 1 to $10^3$ $s^{-1}$, and rolling, brushing, and spraying are on the order of $10^3$ to $10^5$ $s^{-1}$ [8]. The target shear rate for this application is in the pumping shear rate region on the order of 1 to $10^2$ $s^{-1}$. During transport of the material and after placement of the material, the material should not level under gravity thus timing drying and balancing initial moisture content are critical for controlling printing characteristics.

Empirical models have been developed to predict the flow characteristics of powder metal pastes for injection molding, however, it has been observed by Gonzalez-Gutierrez that none of the current models provides an accurate prediction of flow characteristics of powder metal solutions. Their observations have shown that different empirical models must be used as binding agents, mixture ratios, temperatures, powder size, powder shape, and shear rates vary. The current empirical models are based on a "rule of mixtures," however, the solutions exhibit a synergistic behavior which does not follow the standard mixing rules and many of them do not consider the effects of wall slippage. Because of this, empirical models cannot be used to interpolate or extrapolate beyond the measured variants. It was also noted that standard rheometers do not provide an accurate measurement of the powder metal pastes but the use of rheometers can provide a qualitative indication of the flow during injection molding.

Mechanical properties of powder metals and thermoplastics are currently being researched such as the materials being used for composite FFF printers with a heated print head [9]. Nikzad et al. have performed flow characterization on 10% Iron filled ABS at elevated temperatures (270°C). In this research, viscosity behavior is modeled as a Power Law, which is typical for non-Newtonian fluids such as plastic flows. ABS (acrylonitrile butadiene styrene) and PLA (polylactic acid) are common materials used in FFF printing but are solid at room temperature and require a heated print head to transform the material into a liquid state for printing. Polymers and polymeric compounds are generically modeled as a Power Law or other non-linear model as shown by Sochi [10] while studies of Metal Injection Molding (MIM) stock have produced very specific models as shown by Gonzalez-Gutierrez. While, modeling flow rates for these materials analytically is not always accurate, Nikzad was able to recreate flow conditions numerically with some success for PVA based filament [11].

Hong et al. use PVA and polyvinyl carboxy, water, PVA, and sodium hydroxide mixed with copper powder to characterize a 50, 55, 60, and 65% by weight Cu paste [12]. Viscosity was modeled linearly using the Hagen-Poiseuille equation without correction for wall shear effects. As the application calls for low shear stress and low viscosity, this may have been valid due to the range of shear stress applied to the material as certain portions of the pressure/shear curve are linear.

Other research such as Hausnerová et. al. [13] have focused their work on the rheology of powder injection molding (PIM) which focuses on extremely high shear strains of polymer binders. It can be shown that even if the binding agent exhibits Newtonian flow, when mixed with powdered metals, the so-called Newtonian plateau reduces or disappears altogether. Casson or Herschel-Bulkley models have been used to characterize the flow in these applications.

This research attempts to characterize a PVAC/metal paste flow at room temperature for FFF. The off-the-shelf PVAC used is pre-emulsified by the manufacturer which dries in the presence of air thus the mixture must either be composed directly before use or air purged before storage. The feed rates of this mixture in the FFF application do not require high shear stresses and can, for the most part, be modeled linearly. The paste also flows freely at room temperature and therefore, is not directly comparable with much of the research that has been performed. One other added complexity is, given the desired print resolution, capillary losses must be accounted for. Ignoring entrance effects, Mooney Weissenberg Rabinowitsch (MWR) equations will be used to account for wall slip and non-linear effects.

Technology for printing polymer-metal mixtures using heated extruder heads and filled plastic filaments is currently being investigated for desktop printers to bring metal FFF printing to the masses. This approach results in high amounts of binding agent, specialized feedstock, and lower volume of powder in the final components. The purpose of this research is to determine if powder metal components can be produced by FFF at room temperature while maximizing the powder metal composition in the mixture. This will require a 2-phase mixture that is initially fluid at room temperature but hardens quickly upon extrusion. This approach is being used to print concrete structures using FFF [14]. The material characteristics of interest to 3D concrete printing (3DCP) are open time (or operational window of the material as it is time sensitive), setting/layer time, deformation of material as successive layers are added, and material rheology which are identical to this research [15].

A couple advantages of this methodology are that the material can be made inexpensively from off-the-shelf items and the technology required to produce the final parts is inexpensive while maintaining the same strength as cast or forged parts. The ratios of the binding agent, emulsifier, and powdered metal are critical then to generating rheological characteristics that enable the final mixture to flow correctly, maintaining a specified flow rate, and solidify quickly while, ultimately, maximizing the strength of the final material.

As hydration (or dehydration) of the paste contributes to the flow characteristics, one approach to slow dehydration is to mix and capture the paste in a container at the selected hydrated ratio, preventing further dehydration of the binding agent which will aid to control the transport viscosity. During printing the material is driven from this chamber and extruded at a nozzle onto a platform or previous layer.

As specified by Hong and Buswell, the spacing between layers has a significant effect on the composition and therefore the strength of the final matrix. The final extruded component will be subjected to heat treatment to remove the binder and voids between passes and layers of the extruded material. The ratio of binder, emulsifier, and metal powder will also contribute to the final density of the printed material as the emulsifier and binder will be burned out leaving empty pockets in its place. It is then advantageous to minimize the amount of binder and emulsifier in the initial paste.

## Rheological Characterization

The ability to understand the behavior of the material will help to predict the density, flow rates, final material properties, sizing of the printer components, and scalability of printing apparatus. The heat treat process includes burning out the binding agent, leaving behind the metal and voids and porosity where the binder was. The initial density, as governed by the ratios of metals to nonmetal constituents, will contribute to defining the post-print heat treatment process in attempting to remove voids and porosity and define the final material properties. Flow rates are used for predicting the material flow rates through the printer and are used to tune print speeds and feeds. Motor sizing, print head speed and layer height are directly affected by the flow rate and using the wrong density material or incorrect speeds and feeds would be detrimental to the precision, infill, and accuracy of the print. Non-Newtonian fluids do not respond according to standard flow rate models and bridging of the metal particles can cause the fluid to instantaneously solidify if too much pressure is applied to the material by the printer.

Per Gonzalez-Gutierrez, every attempt to create a generic mathematical model for flow of powder metal mixtures for metal injection molding applications was observed to be futile and concluded by showing that modeling flow could be accomplished on a per application and condition basis. Therefore, a generic approach was taken, and test data was fit for this application to the closest models available in the literature. It can be shown that depending on the application, the results from testing fit various models from Newtonian, to Power Law, to shear thinning Visco-Plastic models.

Time independent non-Newtonian fluids are those that exhibit characteristics of both ideal fluids and elastic solids with partial recovery after deformation [16]. The relationship between stress and strain are generally described by the constitutive equation

$$\tau = f(\dot{\gamma}). \qquad 1$$

While this paste is time dependent, for this research, measurements were taken immediately following the initial mixture in an effort to capture comparable results before the interference of dehydration. For high strain rates, such as when pushed through a nozzle, this paste exhibits non-ideal flow and is better defined by Pseudo-Plastics which use a general Power Law model

$$\tau = K(\dot{\gamma})^n \qquad 2$$

where K and n are empirical curve fitting parameters. Most of the material tested remained in the laminar flow region. For those results, the parameter "n" can be approximated for laminar flow as

$$n = \frac{\partial\ ln(\tau)}{\partial\ ln(8u/D)}. \qquad 3$$

$\tau$ and $\dot{\gamma}$ are generally calculated by

$$\tau = \frac{\emptyset \Delta P}{4L} \qquad 4$$

$$\dot{\gamma} = \frac{8u}{\emptyset} = \frac{4Q}{\pi r^3} \qquad 5$$

where L is the length of the nozzle and r is the diameter. The apparent viscosity (μ) for Power Law models is given by the equation

$$\mu = K(\dot{\gamma})^{n-1} = \frac{\tau}{\gamma}. \qquad 6$$

It is observed that using a force-based testing apparatus, the flow characteristics exhibit Visco-plastic behavior. The yield shear stress of Visco-Plastics includes an offset from the origin as a certain amount of energy is required to overcome molecular bonding to begin flow similarly to a Bingham fluid or Casson configuration, which differentiate between a yield shear stress and wall shear stress of which the equations are respectively

$$\dot{\gamma} = \frac{(\tau_w - \tau_0)}{C\prime} \qquad 7$$

$$\dot{\gamma} = \frac{(\tau_w{}^{\frac{1}{2}} - \tau_0{}^{\frac{1}{2}})^2}{K} \qquad 8$$

The previous calculations neglect the effects of wall slip and assume a parabolic flow profile. Alternatively, the MWR equation can be used to approximate the non-Newtonian flow of the paste using the Newtonian flow measurements. For flow characterization that includes wall effects, corrections must be applied to obtain the true wall shear rate using the MWR equation as shown in Equation 9.

$$-\dot{\gamma}_w = \frac{8u}{D}\left[\frac{3}{4} + \frac{1}{4}\frac{d \ln(8u/D)}{d \ln(\tau_w)}\right] \qquad 9$$

where

$\dot{\gamma}_w$ is the true shear rate,
u is the velocity,
D is the diameter of the capillary,
and $\tau_w$ is the wall shear stress.

## Methods

Testing was performed to characterize the metal paste as a Newtonian or non-Newtonian fluid and determine the shear rate flow characteristics of the material which was expected to vary based on the ratios of metal and additives. All testing performed was found to be in the laminar region. For most applications, the material is not expected to exhibit turbulent behavior. First, density was established by measuring a volume and weight of 1 fluid ounce of paste for each mixture.

The force-based setup was performed using a calibrated weight that forced a mixture of paste through an orifice. The test setup consisted of a plunger that accepted a variety of calibrated weights applied to the top. The weights pushed the plunger through a 0.981” diameter chamber forcing the paste out of a 0.1” diameter orifice. The paste was collected in a container and the time required to empty the chamber was recorded. The process was repeated three times for each mixture and an average taken. This information was used to calculate the flow rate, true shear stress, and strain rate. Two mixes of 316 and one mix of carbon steel were tested using this method. To reduce measurement error and automate the process, a secondary, pressure-based setup was established.

The test apparatus for flow rate measurements consisted of paste within a container with inner diameter of 2 inches and exit orifice of 0.10 inches. A calibrated pressure was applied forcing the paste to flow through a capillary. The paste was captured in a container and weighed. The pressure ranged from 2psig to 20psig. The volumetric flow rate (Q) was then calculated using the density and mass flow rate. The wall shear stress and strain rate were calculated and the true shear rate calculated using the MWR equation. This was justified as during the testing, due to transparency of the exit tube, slip at the wall can be visually observed. The true stress and strain are calculated to provide a generic formulation of the paste under five different configurations, four with 316 spherical powder and one with irregular carbon steel powder.

For pressure based testing, all mixes were initially extruded through a constant cross section tube with no nozzle over a constant time interval, then a nozzle was added and the flowrate of mixture 2 was measured through a reduced diameter nozzle to observe the effect of flow path change on rheological characteristics of the fluid. As stated by Gonzalez-Gutierrez, interpolation and extrapolation from this data are not meaningful so exact sizes of nozzles would need to be tested independently to capture the flow characteristics of that specific configuration. Initially, when the nozzle was added, the powdered metal seized and the flow stopped due to the spatial arrangement compacting into a solid suspension. If a smaller size diameter was to be used, the solution would need to be diluted to reduce the percentage of powder in the mixture. The nozzle diameter was then incrementally increased until flow resumed.

## Material Characterization and Results

Figure 1 shows the mixtures for two types of powder used for characterization testing, an irregular powder (10-100µm carbon steel) shown in Figure 1A, and the other spherical (15-45µm 316L) presented in Figure 1B. The irregular carbon powder was provided by a manufacturing company specializing in compression molding thus the powder was premixed with additional binding agents. The spherical powder was provided by a powder material supplier and was pure 316L in spherical form. The ratios of powder, PVA, and water are shown in Figure 2 for each mix.

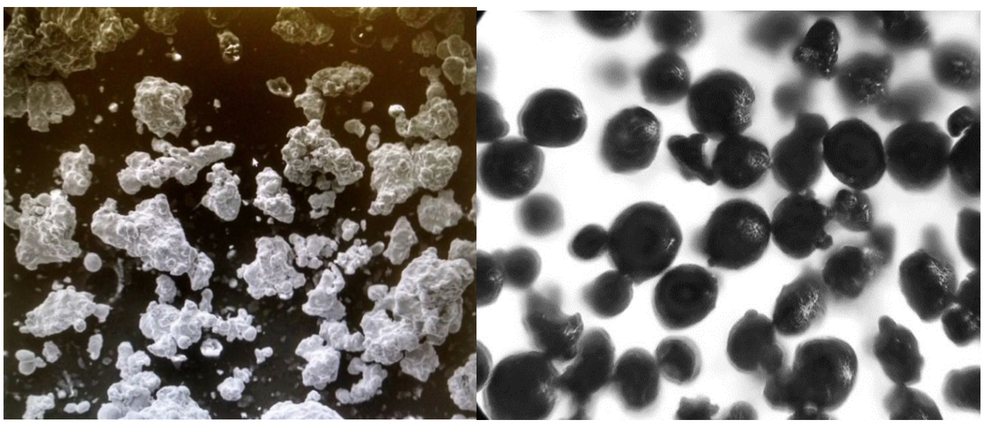

Figure 1A: Irregular Carbon Steel Powder plus Binding Agent @ Left (magnification 485 X).
Figure 1B: Spherical 316L Powder @ Right (magnification 400 X)

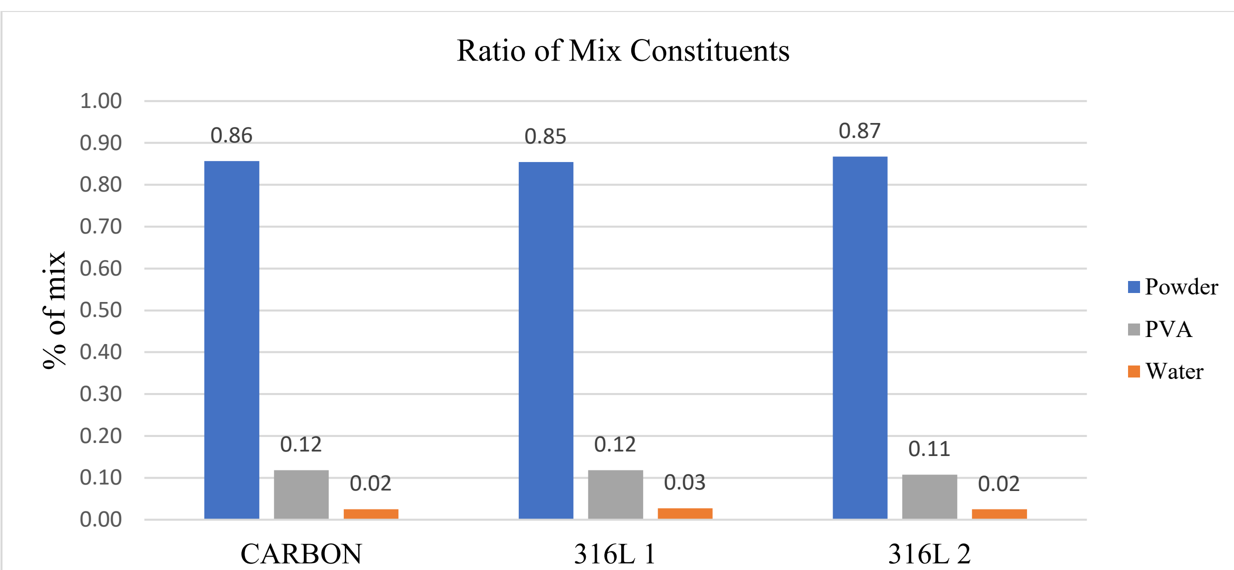


Figure 2 : Ratios by Weight of Powder, PVA and Water per Mix

It was noted that the viscosity of the 316L was lower than that of the carbon steel at higher loads due to the particle size and shape and the binding agent used. The carbon steel paste also solidified after several tens of minutes while the stainless steel remained somewhat pliable after several days. It is assumed this was due to the binding agent already present in the carbon steel that was not present in the stainless powder. Figure 3 contains results of force (lbf) versus volumetric flowrate. As shown in Figure 4, the rheology of Mix 1 can be modeled reasonably well in this region of stress and strain rate as linear. Bingham, Casson, and Power Law models were not applied due to the close fit of the linear model.

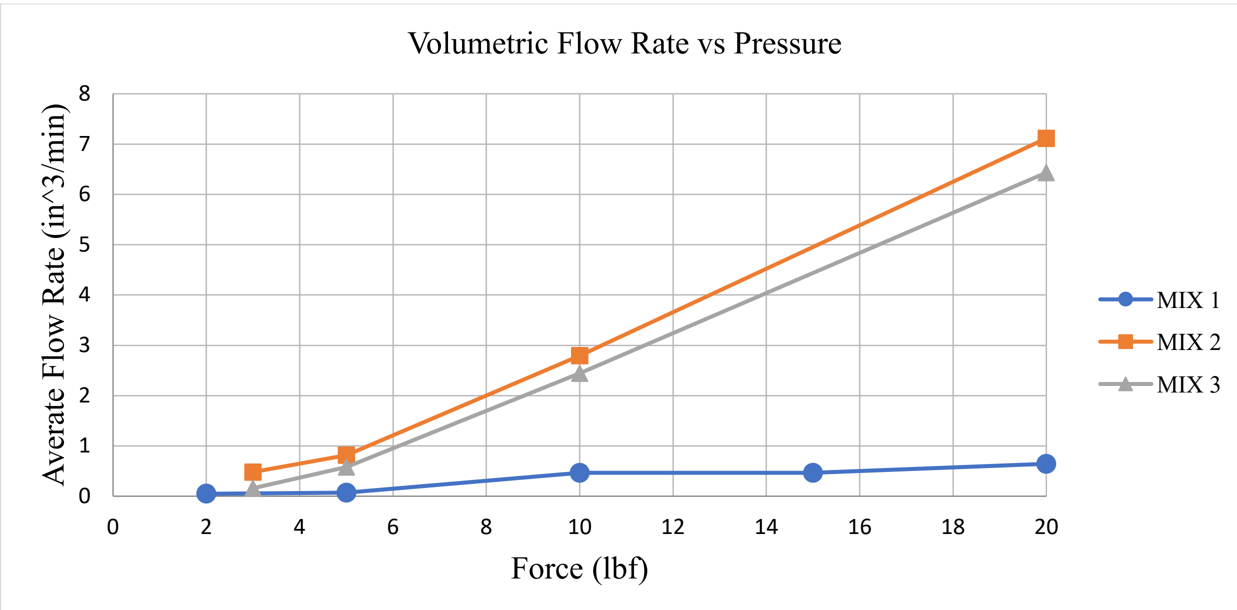


Figure 3: Force Based Flowrate vs Pressure of Mix 1, 2, & 3

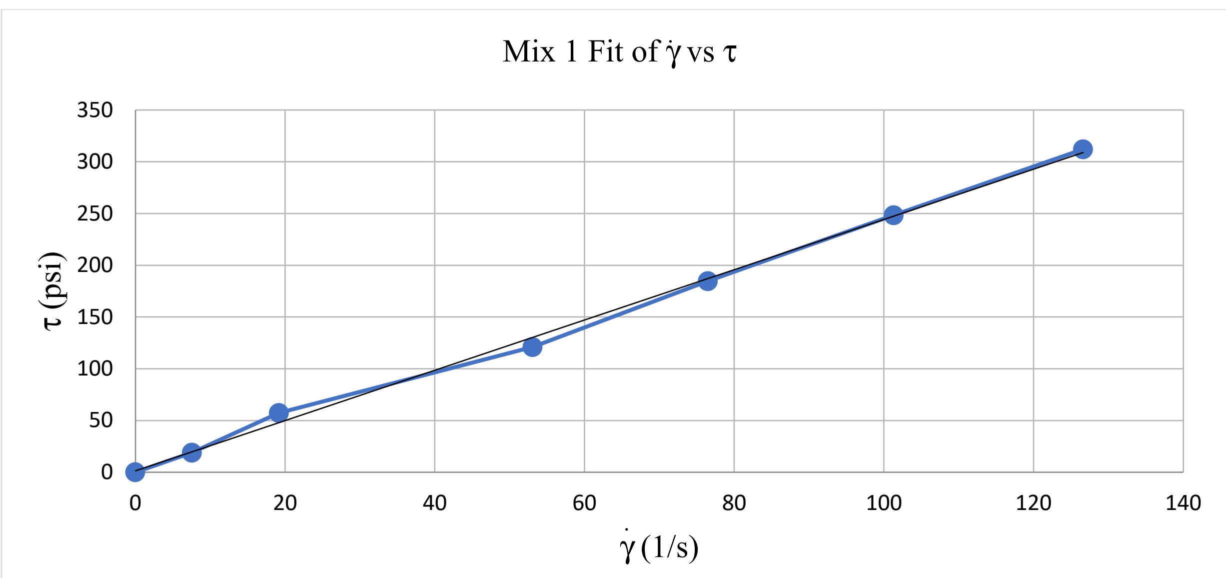


Figure 4: Linear Fit Model of Stress and Strain Rate of Mix 1

The results of testing showed that while mix 1, carbon steel + binding agents and lubricants, behave linearly in this region, the other predominantly metal mixtures exhibit nonlinear behavior as shown by Gonzalez-Gutierrez.

Mixture 2, the first mix of 316L, yielded similar results, however, the final measured $\dot{\varphi}$vs $\tau$ aligned with a power curve model (shown in Figure 5) better than the mix with a higher percent of metal content. While the Power Law provided a better fit for the 316L paste initially, the Casson model provides a more accurate model after the knee of the curve. The fit parameters are shown in Table 1.

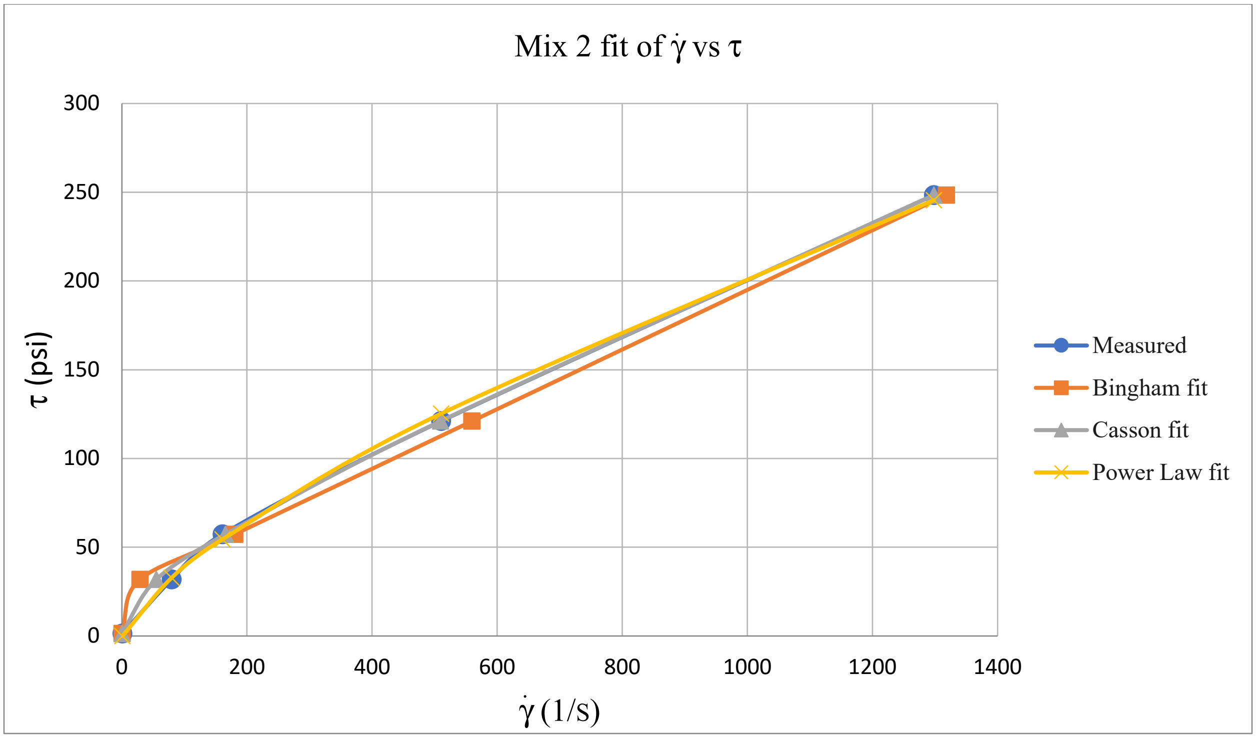


Figure 5: Power, Casson, Bingham Fit Models for the Measured $\dot{\varphi}$vs $\tau$ of Mix 2

Table 1: Bingham, Casson, and Power Law Fit Parameters for Mix 2

| | | | |
|---|---|---|---|
| Bingham | $\tau_0$ = 27 psi | C' = 0.168 | Not a good fit |
| Casson | $\tau_0$ = 9.12 psi | K = 0.125 | Okay fit but departs at the knee |
| Power Law | K=1.3987 | n=0.7209 | Good fit |

The relationships between shear stress and strain rate for the Bingham, Casson, and Power Laws can be found in equations 7, 8, and 2 respectively. Figure 6 shows that the use of a Power Law decently describes the flow for this application initially in the knee of the curve but quickly diverges after.

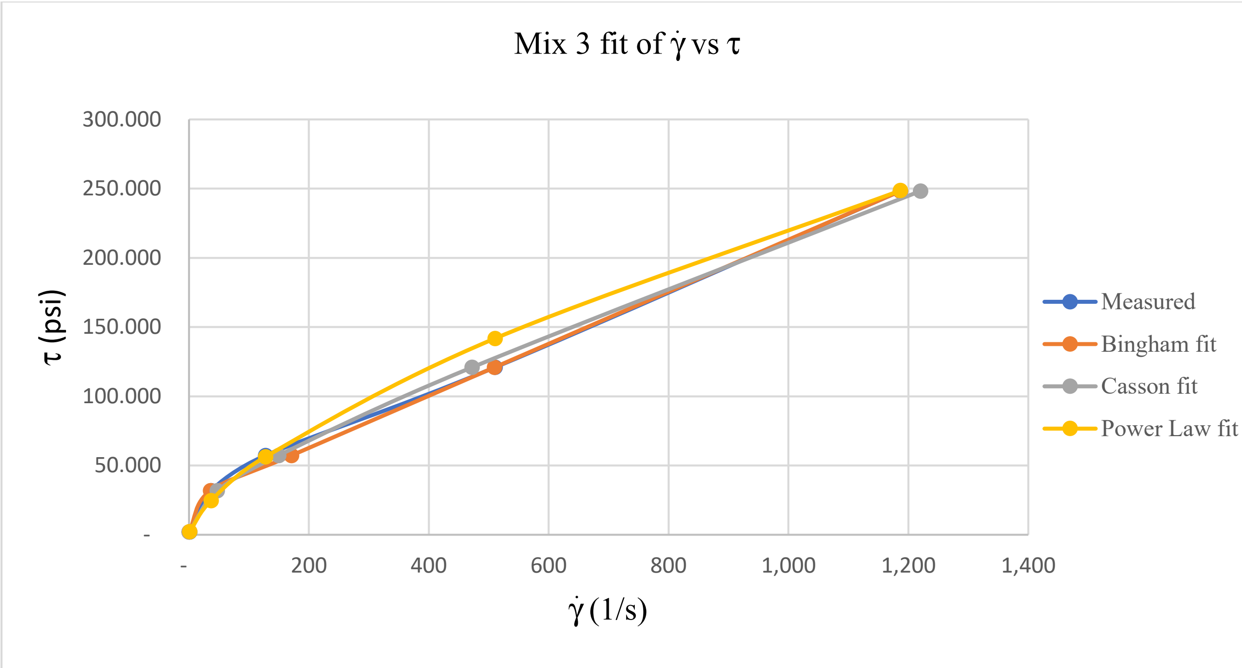


Figure 6: Power, Casson, Bingham Fit Models for the Measured φ̇vs τ of Mix 3

Yield pseudo-plastics include an offset from the origin as a certain amount of energy is required to overcome molecular bonds to begin flow similarly to a Bingham fluid. The fit parameters are shown in Table 2.

Table 2: Bingham, Casson, and Power Law Fit Parameters for Mix 3

| | | | |
|---|---|---|---|
| Bingham | $\tau_0$ = 25.1 psi | C' = 0.188 | Good fit |
| Casson | $\tau_0$ = 10 psi | K = 0.13 | Good fit |
| Power Law | K=2.2365 | n=0.6655 | Not a good fit |

It should be noted at this point that the coefficients C' and K change based on the formulation because there exists no singular model that best describes all flow characteristics. Use of a linear model accurately depicts the first mixture. For the second mixture, a Power Law and Casson approach models flow well, while the Bingham model less accurately describes the flow. For the third mixture, the Bingham and Casson models accurately describe flow while the Power Law is less accurate.

From the pressure-based measurement system, the pressure vs weight extruded testing consisted of four mixes of 316L powder. The ratios of powder, water, and PVA are shown in Figure 7 for each mix. First, the relationship between pressure and extruded weight is shown in Figure 8 and shear stress vs strain rate is provided in Figure 9.

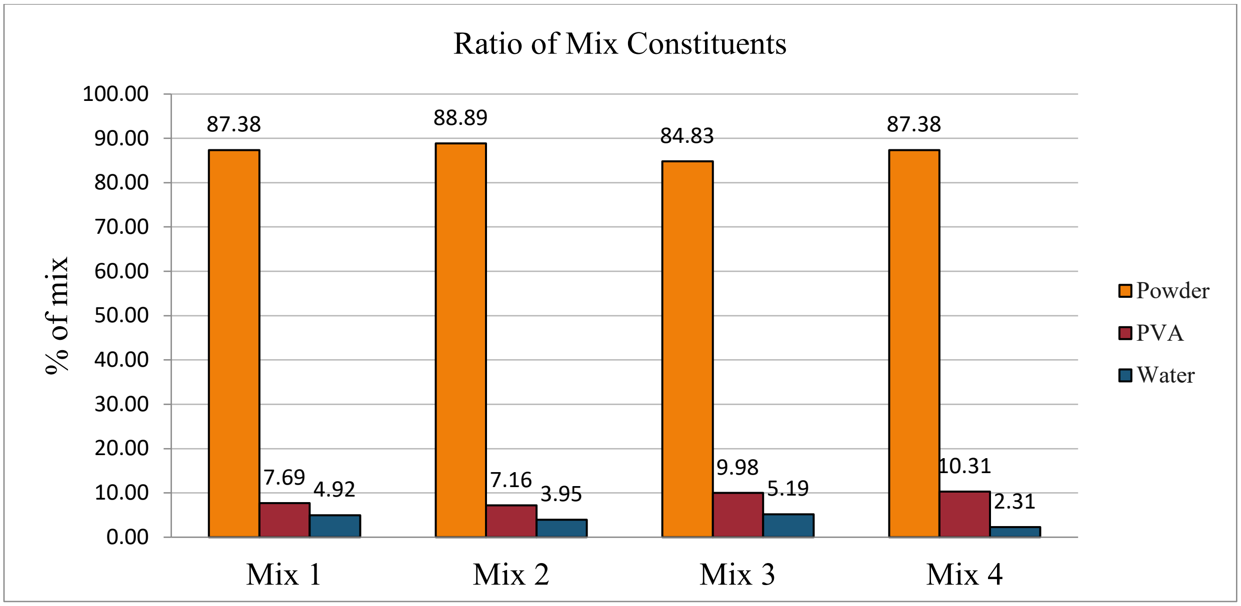


Figure 7: Ratios by Weight of Powder, PVA and Water per Mix

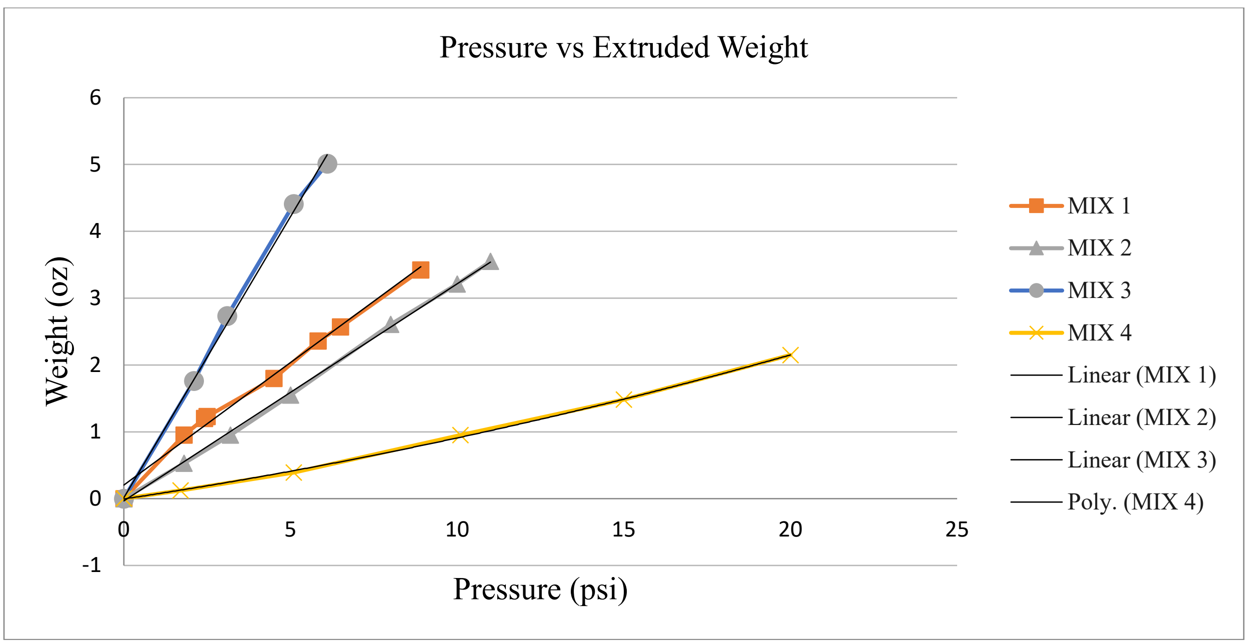


Figure 8: Pressure vs Extruded Weight of Four Mixtures and Curve Fit Models

The first three mixes demonstrate a linear relationship between applied pressure and the flow rate. The last mix, with 2.3% water, began to show a nonlinear relationship between pressure and flow rate. Mixture 4 had the highest viscosity due to the lowest water concentration while mixture 3, which had the highest water concentration, showed the lowest viscosity and given that the third mixture had only slightly less percentage of PVA, suggests that viscosity of the mixture at these approximate percentages is largely dependent upon water content.

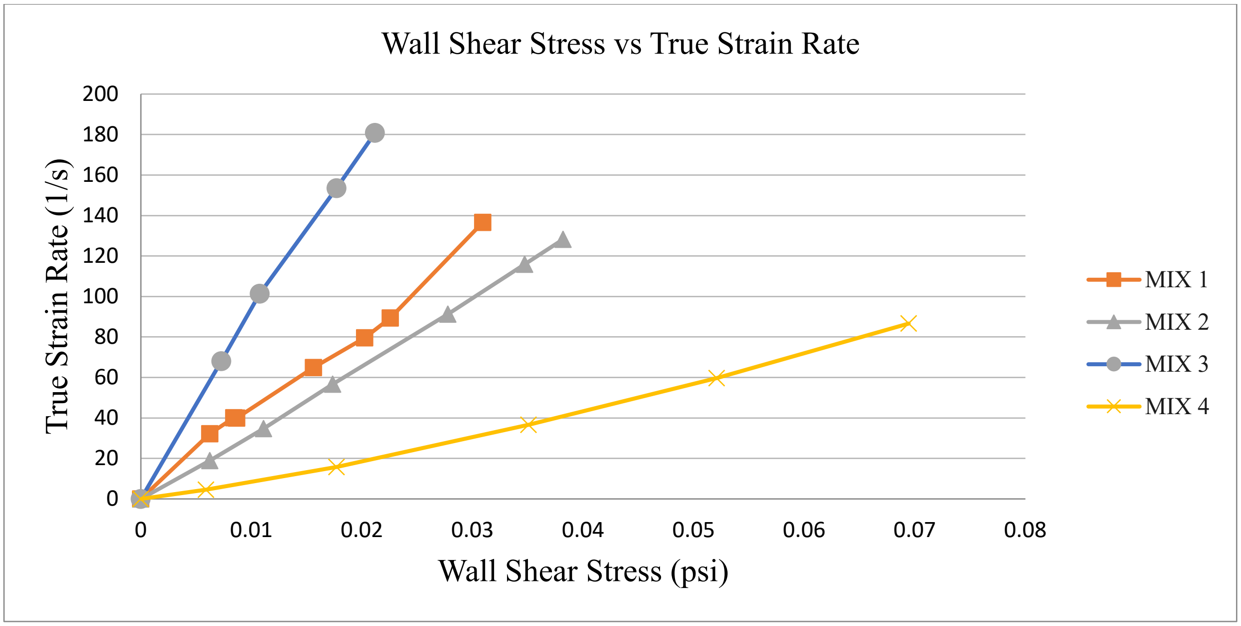


Figure 9: Wall Shear Stress vs True Strain Rate

Figure 10 shows the effect of diameter on the relationship between strain rate and wall shear stress. Additionally, it is believed the nozzle introduced turbulence into the flow as the fluid began to spin upon exiting the nozzle.

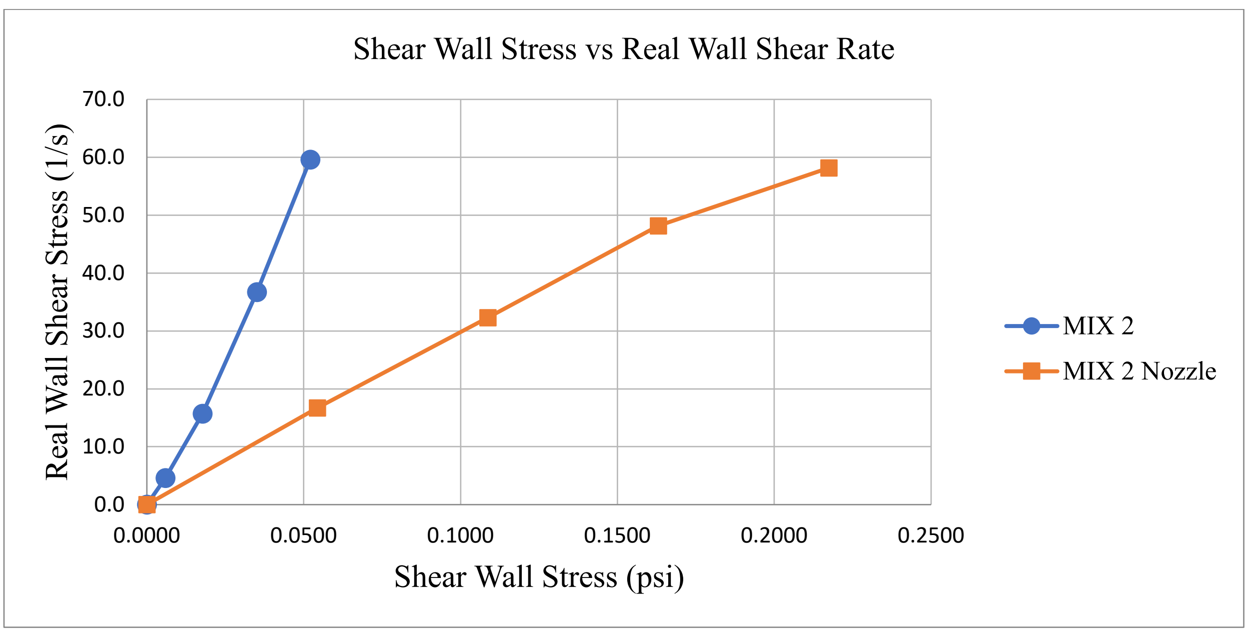


Figure 10: Wall Shear Stress vs True Strain Rate

Because the first three pressure-based measurements fit well into a linear model, over this domain interpolation between mixes may be used somewhat accurately to describe flow behavior. However, as shown by the result of mixture 4, slight changes in the ratios of constituents can lead from linear to nonlinear quickly. Additionally, a change in the diameter of the fluid path will significantly influence the constitutive model.

## Conclusion

In this research, the rheology of varying ratios of powder metal mixtures was investigated. It was observed as suggested by Gonzalez-Gutierrez et al. that a singular model is not sufficient to model all powder-based mixtures but is dependent on application, strain rates, flow geometry, particle size and shape, and mixture ratios of constituents. For this application, it has been shown that using a powder metal-based paste can be used in a similar manner to 3D printed concrete to print components and structures. Interesting observations from this research are that as ratio of powder approaches a solid suspension, the shear stress or pressure required for flow increased rapidly. Secondly, as the nozzle diameter decreased, the constitutive model approached an infinite viscosity, prohibiting flow. From this we can develop a boundary to the limits for applications of powdered metals in FFF.

The next steps include building models that can predict material properties based on flow characteristics, as well as the premix of constituents. Heat treat parameters will be set based on initial ratio of metal to binding agent. Other emulsifiers such as propylene glycol can replace water to ensure that evaporation does not introduce irregularities into the function of the printer but the changes in flowrate or viscosity these new materials introduce must also be understood.

## Bibliography


[1] T. Duda and L. V. Raghavan, "3D Metal Printing Technology," in International Federation of Automatic Control, 2016.

[2] S. Hasanov, S. Alkunte, M. Rajeshirke, A. Gupta, O. Huseynov, I. Fidan, F. Alifui-Segbaya and A. Rennie, "Review on additive manufacturing of multi-material parts: Progress and challenges," Journal of Manufacturing and Materials Processing, vol. 6, page. 4, 2021.

[3] I. Fidan, N. Russell, A. Imeri, C. Ortiz Rios and Y. Chen, "Investigation of the Tensile Properties in Fiber-Reinforced Additive Manufacturing and Fused Filament Fabrication," International Journal of Rapid Manufacturing, vol. 9, 2020.

[4] A. Nasirov and I. Fidan, "Prediction of mechanical properties of fused filament fabricated structures via asymptotic homogenization," Mechanics of Materials, vol. 145, 2020.

[5] I. Fidan, A. Imeri, A. Gupta, S. Hasanov, A. Nasirov, A. Elliott, F. Alifui-Segbaya and N. Nanami, "The trends and challenges of fiber reinforced additive manufacturing," International Journal of Advanced Manufacturing Technology, vol. 102, 2019.

[6] J. Gonzalez-Gutierrez, I. Duretek, C. Kukla, A. Poljšak, M. Bek, I. Emri and C. Holzer, "Models to Predict the Viscosity of Metal Injection Molding Feedstock Materials as Function of Their Formulation," Metals (2075-4701), pp. 1-17, June 2016, Vol. 6, Issue 6.

[7] H.-W. Gao, R. Yang, J. He and L. Yang, "Rheological behaviors of PVA/H2O solutions of high-polymer concentration," Journal of Applied Polymer Science 116(3), pp. 1459-1466, 2010.

[8] A. Uphadayaya, Powder Metallurgy: Science, Technology and Materials, Himiyatnagar, Hyderabad India: Universities Press, 2011.

[9] M. Nikzad, S. H. Masood, S. Igor and A. Groth, "Thermo-mechanical properties of a metal-filled polymer composite for fused deposition modelling applications.," in Proceedings of 5th Australasian Congress on Applied Mechanics., Brisbane, Australia, 2007.

[10] T. Sochi, "Using the stress function in the flow of Generalized Newtonian Fluids Through Pipes and Slits," arXiv:1503.07600, 2015.

[11] M. Nikzad, S. H. Masood, I. Sbarski and A. Groth, "A Study of Melt Flow Analysis of an ABS-Iron Composite in Fused Deposition Modelling Process," TSINGHUA SCIENCE AND TECHNOLOGY ISSN 1007-0214 05/38, Volume 14, Number S1, pp. 29-37, June 2009.

[12] S. Hong, C. Sanchez, H. Du and N. Kim, "Fabrication of 3D Printed Metal Structures by Use of High-Viscosity Cu Paste and a Screw Extruder," Journal of Electrnic Materials Vol. 44, No. 3, 2015.

[13] B. Hausnerova, L. Marcanikova, P. Filip and P. Saha, "Rheological Characterization of Powder Injection Moulding using Feedstock Based on Aluminium Oxide and Multicomponent Water-Soluble Polymer Binder. Recent Advances in Fluid Mechanics and Heat and Mass Transfer," in Proc. of the 9th IASME / WSEAS Int. Conf. on Fluid Mechanics and Aerodynamics, Prague, Czech Republic, 2011.

[14] T. Le, S. A. Austin, S. Lim, R. A. Buswell, A. G. F. Gibb and T. Thorpe, "Mix Design and Fresh Properties for High Performance," Materials and Structures, pp. 1221-1232, 2012.

[15] R. Buswell, "Cement and Concrete Research (2018)," 6 5 2018. [Online]. Available: https://doi.org/10.1016/j.cemconres.

[16] Q.-H. Nguyen and N.-D. Nguyen, Incompressible Non-Newtonian Fluid Flows, Continuum Mechanics - Progress in Fundamentals and Engineering Applications, Dr. Yong Gan (Ed.), ISBN: 978-953-51-0447-6: InTech, 2012.